DOE/NASA/1011-78/29
NASA TM-78956

COLD-AIR PERFORMANCE OF FREE POWER TURBINE DESIGNED FOR 112-KILOWATT AUTOMOTIVE GAS-TURBINE ENGINE

III - EFFECT OF STATOR VANE END CLEARANCES ON PERFORMANCE

Milton G. Kofskey and Kerry L. McLallin
National Aeronautics and Space Administration
Lewis Research Center

December 1978

Prepared for
U. S. DEPARTMENT OF ENERGY
Office of Conservation and Solar Applications
Division of Transportation Energy Conservation

NOTICE

DOE/NASA/1011-78/29
NASA TM-78956

COLD-AIR PERFORMANCE OF FREE POWER TURBINE DESIGNED FOR 112-KILOWATT AUTOMOTIVE GAS-TURBINE ENGINE

III - EFFECT OF STATOR VANE END CLEARANCES ON PERFORMANCE

Milton G. Kofskey and Kerry L. McLallin
National Aeronautics and Space Administration
Lewis Research Center
Cleveland, Ohio 44135

December 1978

Prepared for
U. S. Department of Energy
Office of Conservation and Solar Applications
Division of Transportation Energy Conservation
Washington, D. C. 20545
Under Interagency Agreement EC-77-A-31-1011

SUMMARY

An experimental investigation of a free power turbine designed for a 112-kW, automotive, gas-turbine engine was made to determine the penalty in performance due to the stator-vane end clearances. Tests were made over a range of mean section stator-vane angles from 26° to 50° (as measured from the plane of rotation) with the vane end clearances filled. These results are compared with test results of the same turbine with vane end clearances open.

At design equivalent values of rotative speed and pressure ratio and at a vane angle of 35°, the mass flow with the vane end clearances filled was about 8 percent lower than mass flow with vane end clearances open. This decrease in mass flow was mitigated by increasing the vane angle. This was as expected since vane loading and reaction decrease with increasing vane angle. With the vane end clearances filled, there was about a 66-percent reduction in mass flow when the vane angle was decreased from 40° to 26°. For the same decrease in vane angle the stator throat area decreased by about 50 percent. This result indicates that the rotor losses were increasing with decreasing vane angle.

At design equivalent values of speed and pressure ratio, there was a penalty of about 4 points in total efficiency due to the vane end clearances of 1.1 and 1.9 percent of the vane height for the hub and tip sections, respectively. This penalty remained about constant over the range of vane angles investigated.

Significant increases in total efficiency were obtained for both stator-vane end configurations as the vane angle was increased from 26°. A peak total efficiency of about 0.91 was obtained at the vane angle of 45° with the vane end clearances filled.

Results of static-pressure measurements and rotor-exit surveys showed that the rotor reaction was positive from hub to shroud for the vane angle of 45°. Although high negative rotor incidence angles were obtained, the high positive rotor reactions would be expected to minimize the effects of increased losses due to incidence.

INTRODUCTION

The Department of Energy (formerly the Energy Research and Development Administration) is conducting a program to demonstrate a gas-turbine-powered automobile that meets the 1978 Federal Emissions standards with acceleration characteristics and fuel economy that are competitive with conventionally powered vehicles.

One part of this program involves the performance evaluation of the existing "baseline" sixth-generation gas-turbine engine, which was designed and fabricated by the Chrysler Corporation (ref. 1). The engine has a design power of 112 kilowatts and is used in a 2000-kilogram vehicle. Another part of this program involves cold-air tests of the baseline engine turbomachinery in component test rigs. This report describes cold-air tests conducted on the free power turbine, which uses a variable stator for vehicle braking and engine control. The cold-air performance evaluation of the power turbine has been made with a design, mean-section, vane-chord setting angle of 35° (as measured from the plane of rotation). Results of this performance evaluation are reported in reference 2. Since the vanes are adjustable, performance tests also have been made over a range of vane angles from 26° to 107° (ref. 3).

The objective of the present investigation was to assess the performance penalties caused by the use of vane end clearances, which are required to make the vane adjustable. To accomplish this objective, cold-air tests were made with the vane end clearances filled, and the results were compared with those of reference 3 (vane end clearances open).

Tests for this investigation were made over a range of vane angles from 26° to 50°. These tests were made with an inlet total pressure of about 0.42 bar and a nominal inlet temperature of 303 K. At these conditions design Reynolds number is established at equivalent design values of speed and pressure ratio at the design vane angle of 35°. Data were obtained over a range of speeds and pressure ratios at each vane angle.

Results for both filled and open vane end clearance configurations are given in terms of power, mass flow, and efficiency. The results of rotor-exit radial surveys of absolute flow angle and total pressure for vane angles of 35° and 45° are also presented.

SYMBOLS

A	area, cm^2
$\mathcal{A}$	aspect ratio, b/c
b	blade or vane height, cm
c	blade or vane chord, cm
Δh	specific work, J/g
P	power, kW
p	absolute pressure, bar
R	gas constant, J/kg·K

R_x blade reaction $\left(W_4^2 - W_3^2\right)/2U\Delta V_u$

r radius, cm

s blade spacing or pitch, cm

T temperature, K

U blade velocity, m/sec

V absolute gas velocity, m/sec

W relative gas velocity, m/sec

w mass flow, kg/sec

α absolute gas-flow angle measured from axial direction, deg

β relative gas-flow angle measured from axial direction, deg

γ ratio of specific heats

δ ratio of inlet total pressure to U.S. standard sea-level pressure, p_2'/p^*

ϵ $= (0.740/\gamma)\ (\gamma + 1/2)^{\gamma/(\gamma-1)}$

η turbine efficiency

θ_{cr} $= \left(V_{cr}/V_{cr}^*\right)^2$

κ vane exit angle, deg (see fig. 2(b))

σ solidity, c/s

ψ mean section vane chord setting angle (or vane angle), deg (see fig. 2(b))

ω turbine speed, rad/sec

Subscripts:

cr condition corresponding to Mach number of unity

des design

eq equivalent

m mean section

t tip

th throat

u tangential

x axial

1 station upstream of prerotation vanes (fig. 5(a))

2 station at vane inlet (fig. 5(a))

3 station at vane exit (fig. 5(a))

4 station at rotor exit (fig. 5(a))

Superscripts:

' absolute total state

* U.S. standard sea-level condition (temperature, 288.15 K; pressure, 1.013 bars)

TURBINE DESCRIPTION

The free power turbine was designed to deliver 112 kilowatts in a 2000-kilogram automotive vehicle. The salient design parameters are listed in table I. Design-point parameters (corresponding to the 100 percent power point) are given at design inlet pressure and temperature. Air-equivalent, as well as test, conditions are also given.

Figure 1 is a cross section of the power-turbine test package. Engine hardware such as the interstage duct, variable-stator assembly, rotor assembly, turbine-exit diffuser and bearing assembly were used to build up the test package.

Stator Assembly

The variable stator for the power turbine was designed to provide for vehicle braking and engine control. This requires that the vanes rotate through large arcs. To minimize stator-vane end clearances, the stator endwalls were designed to be concentric, spherical surfaces. With the pivot axis of the variable stator chosen to lie on a line passing through the center of the spherical surfaces, the hub and tip end clearances were constant for all vane angles. The average measured vane end clearances were 0.025 and 0.041 centimeter for the hub and tip, respectively. These clearance values are 1.1 and 1.9 percent of the passage height for the hub and tip, respectively.

The stator assembly (fig. 2(a)) consists of 27 vanes. The vane has changing cross section, twist from hub to tip, and an aspect ratio of 0.828 based on mean section chord. The main stator aerodynamic parameters are given in table II. The vane pivot shank was modified by incorporating an O-ring on the shank to prevent air leakage from the vane passages to the exit collector along the shank. The air leakage through the shank was minimized for two reasons. First, the results are presented in terms of blading efficiency, which does not include losses due to friction of bearings and seals nor any loss due to leakage along the blade shank. Second, losses resulting from this leakage would have a larger effect on performance in the cold-air performance tests than actual

operation in the engine at the higher pressures and temperatures. The angle between the vane mean-section chord line and the plane of rotation is defined as the vane angle. The design vane angle was 35°. The effect of vane angles of 26°, 35°, and 45° on the flow passage is shown in figure 2(b). The variation of stator throat area and mean-section vane-exit-camber-line angle with vane angle are shown in figures 2(c) and (d). It can be seen that, above the design vane angle (35°), a 5°-vane-angle change results in about a 20-percent change in vane throat area and that, below the design vane angle, a 5°-vane-angle change results in a slightly greater than 20-percent change in vane throat area.

Rotor

The rotor has 51 blades and an aspect ratio of 1.393, based on the mean blade height and the mean-section actual blade chord. The rotor has a constant hub diameter of 14.163 centimeters, and the tip diameter increases from 18.753 to 18.966 centimeters through the blade row. The nominal radial tip clearance was 0.046 centimeter, which is about 2 percent of the mean annular passage height. The rotor-blade profile has a changing cross section and twist from hub to tip. The rotor is shown in figure 3, and the main rotor aerodynamic parameters are listed in table II.

APPARATUS

The apparatus used in this experimental cold-air investigation consisted of the turbine test package, an airbrake dynamometer to absorb the power and measure the torque output of the turbine, and an inlet and exhaust piping system with flow-control valves. The arrangement of the apparatus and a photograph of the turbine test apparatus are shown in figure 4. Pressurized air was used as the driving fluid for the turbine. The air was piped into the turbine through a filter, a mass-flow measuring station (consisting of a calibrated flat-plate orifice), and a remotely controlled pressure-regulating valve. The air, after passing through the turbine, was exhausted through a remotely operated valve into a central low-pressure exhaust system.

A row of prerotation vanes was installed in the inlet section of the interstage duct (figs. 1 and 5(a)) to simulate the whirl that is imparted to the air by the compressor-drive turbine in the engine.

The airbrake dynamometer was cradle-mounted on air bearings for torque measurement. The force on the torque arm was measured with a commercial strain-gage load cell. The rotational speed was measured with a magnetic pickup and a shaft-mounted gear.

INSTRUMENTATION

Turbine performance was determined by measurements taken at stations 2 and 4. (See fig. 5(a) for station locations.) Turbine-inlet total temperature was taken at station 1 and was assumed to be the same at station 2. Thermocouple rakes could not be installed at station 2 because it would have involved drilling through several mating parts (see fig. 1). At station 1 the instrumentation consisted of four total-temperature rakes spaced at 90° intervals around the circumference. Each rake contained three thermocouples at the center radii of three equal annular areas. At stations 2 and 3 (stator inlet and exit) there were eight wall-static-pressure taps, four each on the inner and outer walls. These inner- and outer-wall taps were located opposite each other at 90° intervals around the circumference and at the projected midflow passage for the 35° vane angle.

At station 4, approximately one mean-section-axial-chord length downstream of the rotor trailing edge (1.6 cm), the static pressure, total pressure, total temperature, and flow angle were measured. The static pressure was measured with eight wall taps, four each on the inner and outer walls. These inner- and outer-wall taps were located opposite each other at 90° intervals around the circumference. Three radially actuated, self-alining claw-shaped probes were located circumferentially, 90° apart. These probes were used for the simultaneous measurement of rotor-exit total pressure, total temperature, and flow angle at three radial positions in the passage. Figure 5(b) is a photograph of the probe actuator, the balance capsule (for self-alinement), and the claw-shaped probe. Figure 5(c) is an enlarged photograph of the probe head showing the thermocouple, total-pressure tube and the two tubes for angle measurement.

Absolute pressures at the various stations were measured directly with absolute-pressure transducers. The data were recorded by integrating digital equipment.

PROCEDURE

The turbine was operated at nominal stator-inlet total conditions of 303 K and 0.42 bar. These conditions resulted in a Reynolds number that was the same as that for engine operating conditions. Data were obtained over a range of stator-inlet-total- to rotor-exit-static pressure ratios of about 1.13 to 2.58, over a range of speeds from 20 to 130 percent of design, and over a range of vane angles from 26° to 50°.

Before the performance tests, tare torque due to friction of the bearings and seals and windage of the disk and coupling was obtained by measuring the torque required to rotate the shaft and bladeless rotor disk over the range of speeds covered in the investigation. A tare torque of 1.5 newton-meters, which is about 29 percent of the actual turbine torque, was obtained at design equivalent speed and power. During the tare torque

tests, axial thrust loads were applied on the turbine thrust bearing. The results indicated no measurable change in friction in the 0- to 222-newton thrust-load range. The axial thrust loads encountered in the tests ranged from about 0 to 137 newtons. The tare torque was added to the dynamometer torque to obtain turbine blading efficiency.

The turbine was rated on the basis of total efficiency. The total pressures at stations 2 and 4 were calculated from mass flow, static pressure, total temperature, and flow angle from the following equation:

$$p' = p\left\{\frac{1}{2} + \frac{1}{2}\left[1 + \frac{2(\gamma - 1)R}{\gamma}\left(\frac{w\sqrt{T'}}{pA\cos\alpha}\right)^2\right]^{1/2}\right\}^{\gamma/(\gamma-1)}$$

The rotor-exit total temperature T'_4 was derived from the inlet temperature and the enthalpy drop based on torque, mass flow, and speed. The outlet flow angle α_4 was the absolute flow angle measured from the axial direction. The variation of inlet flow angle α_2 with mass flow was obtained from a stator flow check done before the performance tests.

The vane end clearances were filled with a mixture of talcum powder and dope. This mixture was inserted so as to have as small a fillet as possible. The fillet radius was 0.025 to 0.040 centimeter. This process was repeated for each vane setting angle investigated. Detail of the filled vane end clearance is shown in figure 1.

RESULTS AND DISCUSSION

Performance results are presented for a free power turbine designed for a baseline automotive gas-turbine engine, which delivers 112 kilowatts in a 2000-kilogram vehicle. Performance tests were made with air as the working fluid at inlet conditions of about 0.42 bar and an inlet total temperature of about 303 K. These conditions, at equivalent design speed and pressure ratio and at the design vane angle, resulted in a test Reynolds number that was equal to that at actual design operating Reynolds number for the baseline engine. Performance data were obtained with vane end clearances filled over a range of vane angles ψ of 26 to 50°. The results are compared with those of reference 3, which were obtained with the same turbine operating with vane end clearances open. Results in terms of performance and internal flow characteristics are shown herein.

Performance

Mass-flow. - Figure 6 shows the effect of open and filled vane end clearances on mass flow over the range of vane angles from 26° to 50°. The variation of mass flow with vane-inlet-total- to rotor-exit-static-pressure ratio p'_2/p_4 is shown for several values of constant speed. In general, the difference in mass flow between the two configurations (open and filled vane end clearances) decreased with increasing vane angle. This is to be expected because vane loading and stator reaction (static-pressure drop) decrease with increasing vane angle; hence, flow through the vane end clearances would decrease with decreasing loading (decreasing Δp across end clearance). The stator choked at p'_2/p_4's above about 2.0 for vane angles of 26° to 35°. The rotor choked at vane angles of 45° and 50° at higher pressure ratios.

Figure 7 shows the effect of vane angle and vane end clearances on mass flow at design equivalent speed and a design equivalent total-pressure ratio p'_2/p'_4 of 1.680 (which corresponds to an overall design total-pressure ratio of 1.698 including diffuser listed in table I). Mass flow is shown as a fraction of the value obtained at the design vane angle of 35° with the vane end clearances open. This vane angle produced about an 8-percent decrease in mass flow when the vane end clearances were filled. The difference in mass flow between the two configurations decreased with increasing vane angle up to an angle of 45°. The long dashed line in figure 7 shows the stator throat area variation with vane angle. There was about a 50-percent decrease in stator throat area for a reduction in vane angle from 40° to 26°. For the filled configuration a 66-percent reduction in mass flow occurred when the vane angle was decreased from 40° to 26°. This indicates that the rotor losses were increasing at a greater rate with decreasing vane angle than was the throat area. This is readily seen by the greater slope of the mass-flow curve compared with the slope of the throat-area curve.

Performance map. - The performance maps of figure 8 were obtained from cross-plots computed from values selected from smoothed curves of equivalent torque and equivalent mass flow. The performance maps show equivalent power as a function of equivalent-mass-flow - speed parameter. Lines of equivalent rotative speed (as a percent of design), stator-inlet-total- to rotor-exit-total pressure ratio p'_2/p'_4, and total efficiency are shown. Comparison of performance maps for a given vane angle shows the difference in performance between open and filled vane end clearances. The comparison shows a significant improvement in efficiency when the vane end clearances were filled. Further, it can be noted that there was a significant decrease in peak efficiency when the vane angle was decreased from 50° to 26°.

Figure 9 shows the variation of total efficiency as a function of vane angle for design equivalent speed and the design equivalent total-pressure ratio p'_2/p'_4 of 1.680. The dashed line represents the turbine total efficiency with vane end clearances filled, and the solid line represents the turbine total efficiency with vane end clearances open.

There is a significant increase in total efficiency for both vane end clearance configurations as the vane angle ψ was increased. Peak total efficiency of 0.91, for the filled clearance configuration, was obtained for the 45° vane angle. Over the range of vane angles investigated, there was a penalty of about 4 points in total efficiency attributable to effects associated with vane end clearances of 1.1 and 1.9 percent of the vane height at the vane hub and tip sections, respectively. These results, therefore, indicate that for the vane end clearances tested there was a significant efficiency penalty associated with vane end clearances. The change in efficiency penalty with variation in vane end clearances was not assessed. However, it is felt that, at the hub or inner wall where the stator reaction is highest, the penalty in efficiency caused by increases in clearance will be greater. Justification for this statement may be found in investigations of rotor-tip-clearance effects such as reference 4, which shows a greater penalty in efficiency when the rotor is of a reaction design as compared with an impulse design.

Internal Flow Characteristics

Static pressure through turbine. - Figures 10 and 11 show the variation of outer- and inner-wall static pressures through the turbine for operation at design equivalent values of speed and turbine total-pressure ratio. Positive outer-wall rotor reaction (indicated by the decrease in static pressure through the rotor) occurred for both vane end clearance configurations over the entire range of vane angles investigated (fig. 10). There was very little difference in outer-wall rotor reaction between the two stator configurations, particularly for the vane angles of 40° and 45°. At 26° there was an increase in stator reaction for the filled clearance configuration. This result would occur from the reduced mass flow with no change in rotor loss. If there were a reduction in rotor loss (as indicated by higher efficiency), a further increase in stator reaction would occur for the case with vane end clearances filled.

Figure 11 shows the effect of vane end clearance on static pressure along the inner-wall or hub. Negative inner-wall rotor reaction (indicated by a rise in static pressure through the rotor) occurred for both stator configurations for vane angles of 26° to 35°. For the 40°, 45°, and 50° vane angles positive inner-wall rotor reaction was obtained with vane end clearances open, while for the vane angle of 40° there was some negative inner-wall or hub rotor reaction with the vane end clearances filled. It should be noted that, with the exception of the 26° vane angle, stator reaction was larger when the vane end clearances were filled than when they were open. For the 26° vane angle the stator reaction was the same for both configurations. This implies that rotor hub losses in terms of blockage must have increased by the amount that the mass flow decreased when the vane end clearances were filled.

Local total efficiency. - Figure 12 shows the variation of local total efficiency and rotor-exit flow angle with radius ratio at design equivalent speed and turbine total-pressure ratio for the design vane angle of 35° and the two end configurations. The improvement in local total efficiency due to filling in the vane end clearances was obtained primarily along the outer half of the passage height. This probably resulted from the fact that the outer-wall vane end clearance was about 73 percent greater than the hub or inner-wall vane end clearance. The positive rotor-exit absolute flow angles for both end clearance configurations indicate a negative contribution to specific work. It would appear that the improvement in performance along the outer half of the passage height for the vane configuration with end clearances filled was chiefly the result of increase whirl V_u at the inlet to the rotor, since there was very little difference in rotor-exit flow angle in this region for the two end clearance configurations.

Figure 13 shows the variation of local total efficiency and rotor-exit flow angle with radius ratio for the filled clearance configuration at vane angles of 35° (design) and 45° (corresponding to maximum performance) for design-equivalent rotative speed and pressure ratio. The local total efficiency was better for the 45° vane angle than for the 35° vane angle over about 79 percent of the passage height. Reasons for the improvement in total efficiency will be discussed in the following section on velocity diagrams. Negative angles in the rotor-exit absolute-flow-angle curves indicate a positive contribution to work. The plot shows that the exit angle changed from positive for the 35° vane angle to negative for the 45° vane angle over the entire passage height. This resulted from the increase in relative velocity through the rotor as the stator throat area increased with the change in vane angle from 35° to 45°. The wheel speed was the same for both sets of data.

Velocity diagrams. - Velocity diagrams in figures 14 and 15 were calculated from the available survey data. Survey data from tests reported in reference 3 were used to determine the velocity diagrams of figure 14(a). Some assumptions were necessary to compute the velocity diagrams from the available data:

(1) Radially constant stator-inlet total temperature and inlet total pressure

(2) Linear variation in static pressure between measured inner- to outer-wall values for all three measuring stations

(3) Measured mean values of rotor-exit absolute total temperature (from three survey probes) corrected so the mass-averaged specific work matched the specific work as obtained from torque, speed, and mass-flow measurements

(4) Stator total-pressure loss assumed radially constant and adjusted so the integraded mass flow from pressure, temperature, flow angle, and area matched the measured mass flow

Figure 14 shows the velocity diagrams for both vane end clearance configurations at the design vane angle of 35°. Both end clearance configurations show negative hub rotor reactions (as indicated by the decrease in relative critical velocity ratio W/W_{cr} through

the rotor). The velocity diagrams of figure 14 indicate low mass flow (low $(V_x/V_{cr})_4$) along the hub or inner wall. This may be the result of the combined effect of high incidence angle and high negative reaction causing high total-pressure loss, which would allow secondary flows to develop and possibly cause flow separation. This will be shown in the discussion of table III.

Subsonic flow occurred through all sections of the stator and rotor for both end clearance configurations. These subsonic velocities, therefore, indicate that neither the stator nor the rotor was choked at design-equivalent speed and work.

Figure 15 shows the calculated velocity diagrams for the 45° vane angle with the vane end clearances filled. This was the vane angle at which the highest turbine efficiency was obtained at design-equivalent speed and pressure ratio. The velocity diagrams indicate positive rotor reaction (increase in relative critical velocity ratio W/W_{cr} through the rotor). This would be expected to result in lower rotor losses at the hub when compared with the results for both stator clearance configurations at the 35° vane angle. Again, the velocities through the turbine are subsonic. Notice that there was essentially uniform flow from hub to tip at the exit to the rotor.

Table III summarizes the main aerodynamic parameters for the open and filled vane end clearances at the 35° vane angle and for the filled vane end clearances at the 45° vane angle. A comparison of the deviation angles listed in table III shows that there was considerable underturning of the flow at the stator-exit hub section for both vane end clearance configurations with the 35° vane angle. Considerable overturning of the flow at the rotor-exit hub section was obtained for both end clearance configurations with the 35° vane angle. This overturning suggests a strong passage vortex. The absence of overturning at the rotor tip or outer wall could have resulted from the interaction of rotor-tip leakage counteracting the effect of a passage vortex on the flow.

Considerable negative rotor incidence angles were obtained at the hub for both end clearance configurations and for all vane angles investigated. Based on the results of Ainley and Mathieson (ref. 5), high negative rotor incidence at the hub section for the 35° vane angle and open end clearances could result in about a 30-percent increase in blade profile loss when compared with that obtained at an optimum incidence value.

Negative rotor reaction was obtained at the rotor hub for both end clearance configurations with the 35° vane angle. Reference 6 indicates that, for an ideal rectangular form of loading diagram, negative reaction results in increased total blade-surface diffusion. Increased total blade-surface diffusion will result in high blade-profile loss. The combination of high rotor incidence and high negative rotor reaction could result in excessive blade profile losses with possible flow separation at the hub section. Although there was high negative rotor incidence for the 45° vane angle, high positive rotor reaction would be expected to minimize the effects due to incidence. Note that high positive rotor reactions were obtained at all radial sections for the 45° vane angle.

As was mentioned previously, the improvement in performance, when the vane end clearances were filled for the 35° vane angle was the result of increased stator-exit whirl. A comparison of the exit whirl $(V_u/V_{cr})_3$ (table III) shows that the larger increase in whirl occurs at the mean and tip sections.

The radial variation in mass flow at the rotor exit is indicated by the variation in the axial velocity component $(V_x/V_{cr})_4$. As stated previously, low mass flow was obtained at the rotor-exit hub section for both vane end configurations with the 35° vane angle. Comparatively uniform rotor-exit flow was obtained from hub to tip for the 45° vane angle as shown by the axial-velocity component. The contributing factors for peak efficiency being obtained at this vane setting angle was high rotor reaction and a favorable flow field from hub to tip, as indicated by the stator and rotor deviation angles and the uniform rotor-exit flow.

SUMMARY OF RESULTS

An experimental investigation was conducted on a baseline power turbine designed for a 112-kilowatt automotive gas turbine engine. Cold-air tests were made with the variable stator vane end clearances filled. To determine the penalty in performance due to the stator vane end clearances, these results are compared with those obtained with the stator vane end clearances open. Tests were made over a range of vane angles from 26° to 50° as measured from the plane of rotation. Results of this investigation at design equivalent values of rotative speed and pressure ratio may be summarized as follows:

1. At design vane angle of 35°, there was about an 8 percent decrease in mass flow when the vane end clearances were filled.

2. The effect of vane end clearances on mass flow decreased with increasing vane angle. This was to be expected because vane loading and reaction decreases with increasing vane angle.

3. There was a reduction of about 66 percent in mass flow when the vane angle was decreased from 40° to 26° with vane end clearances filled. The stator throat area decreased by about 50 percent for the same decrease in vane angle. This indicates that the rotor losses were increasing at a greater rate with decreasing vane angle than was the throat area.

4. Over the range of vane angles investigated, there was a penalty of about 4 points in total efficiency as a result of vane end clearances of 1.1 and 1.9 percent of vane height at the vane hub and tip, respectively.

5. Significant increases in turbine total efficiency were obtained as the vane angle was increased from 26°. Peak total efficiency of about 0.91 was obtained at the vane angle of 45° with vane end clearances filled.

6. Results of static-pressure measurements and rotor-exit-total-pressure survey measurements on the filled configuration showed that, for the 45° vane angle, high positive rotor reactions were obtained at all radial sections. The contributing factors for peak efficiency being obtained at this vane setting angle was high rotor reaction and a favorable flow field from hub to tip as indicated by the stator and rotor deviation angles and the uniform rotor-exit flow.

Lewis Research Center,
National Aeronautics and Space Administration,
Cleveland, Ohio, August 22, 1978,
778-32.

REFERENCES

1. Angell, P. R.; and Golec, Thomas: Upgrading Automotive Gas Turbine Technology, An Experimental Evaluation of Improvement Concepts. SAE Paper 760280, Feb. 1976.

2. Kofskey, Milton G.; and Nusbaum, William J.: Cold-Air Performance of Free Power Turbine Designed for 112-Kilowatt Automotive Gas-Turbine Engine. I - Design Stator-Vane-Chord Setting Angle of 35°. NASA TP-1007, 1978.

3. McLallin, Kerry L.; and Kofskey, Milton G.: Cold-Air Performance of Free Power Turbine Designed for 112-Kilowatt Automotive Gas-Turbine Engine. II - Effect of Variable Stator-Vane-Chord Setting Angle on Turbine Performance. NASA TM-78993, 1978.

4. Haas, Jeffrey E.; and Kofskey, Milton, G.: Cold-Air Performance of a 12.766-Centimeter-Tip-Diameter Axial-Flow Cooled Turbine. III - Effect of Rotor Tip Clearance on Overall Performance of a Solid Blade Configuration. NASA TP-1032, 1977.

5. Ainley, D. G.; and Mathieson, G. C. R.: Examination of the Flow and Pressure Losses in Blade Rows of Axial-Flow Turbines. R. & M. No. 2891, British ARC, 1955.

6. Stewart, Warner L.; Whitney, Warren J.; and Wong, Robert Y.: A Study of Boundary-Layer Characteristics of Turbomachine Blade Rows and Their Relation to Over-All Blade Loss. J. Basic Eng., vol. 82, Sep. 1960, pp. 588-592.

TABLE I. - TURBINE DESIGN POINT PARAMETERS

Parameter	Engine operation	Equivalent conditions	Test conditions
Inlet temperature, K	1104.2	288.2	303.0
Inlet pressure, bar	1.894	1.01	0.42
Mass flow, kg/sec	1.001	1.075	0.436
Rotative speed, rpm	35 845	18 534	19 004
Specifc work, Δh, J/g	112.5	30.2	31.7
Mean rotor tip diameter, D_m, cm	16.511	16.511	16.511
Work factor, $\Delta V_u/U_m$	1.172	1.172	1.172
Total efficiency (including diffuser), η	0.742	0.742	.742
Total-pressure ratio (including diffuser)	1.661	1.698	1.698
Power, kW	112.5	32.3	13.8

TABLE II. - TURBINE BLADING PARAMETERS

Blade row	Section	Solidity,[a] σ	Aspect ratio,[a] $\mathscr{A}$	Reaction,[a] R_x	Number of blades	Clearance	
						cm	Percent passage height
Stator	Hub	1.49	-----	------	27	0.025	1.1
	Mean	1.53	0.828	------	27	-----	---
	Tip	1.56	-----	------	27	.041	1.9
Rotor	Hub	1.98	-----	-0.160	51	-----	---
	Mean	1.65	1.393	.195	51	-----	---
	Tip	1.44	-----	.339	51	0.046	2.0

[a]See SYMBOLS for definition.

TABLE III. - TURBINE AERODYNAMIC PARAMETERS

Vane angle, ψ deg	Vane end clearance	Blade row	Blade section	Exit deviation angle, deg (a)	Incidence angle, [b] deg	Reaction, [c] R_x	Exit whirl, $(V_u/V_{cr})_3$	Axial velocity component, $(V_x/V_{cr})_4$
35	Open	Stator	Hub	-10.0	-----	------	0.797	-----
			Mean	+.3	-----	------	.766	-----
			Tip	-3.4	-----	------	.661	-----
		Rotor	Hub	+17.6	-15.1	-0.160	-----	0.194
			Mean	-6.6	+4.8	.195	-----	.372
			Tip	-4.7	-3.6	.339	-----	.355
35	Filled	Stator	Hub	-9.8	-----	------	0.840	-----
			Mean	+4.2	-----	------	.820	-----
			Tip	+3.6	-----	------	.723	-----
		Rotor	Hub	+20.8	-13.3	-0.208	-----	0.136
			Mean	-1.5	+14.3	.024	-----	.313
			Tip	-6.8	+10.6	.178	-----	.371
45	Filled	Stator	Hub	+0.6	-----	------	0.707	-----
			Mean	0	-----	------	.613	-----
			Tip	-5.4	-----	------	.501	-----
		Rotor	Hub	-2.0	-19.2	0.366	-----	0.421
			Mean	+.4	-17.5	.606	-----	.460
			Tip	+2.1	-26.2	.697	-----	.450

[a] Minus signs indicate underturning; plus, overturning.

[b] Incidence is the blade-inlet-flow angle minus the blade-inlet angle.

[c] See SYMBOLS for definition.

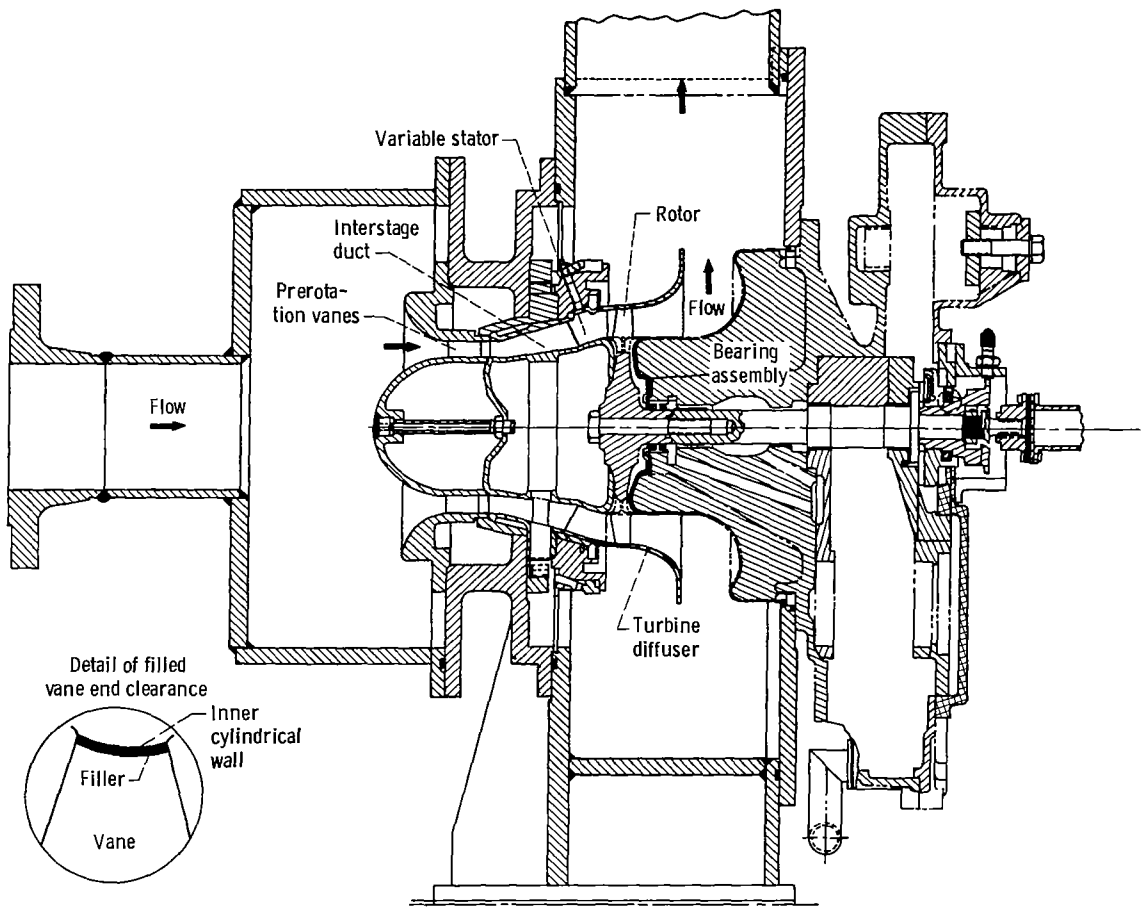

Figure 1. - Cross section of turbine test package.

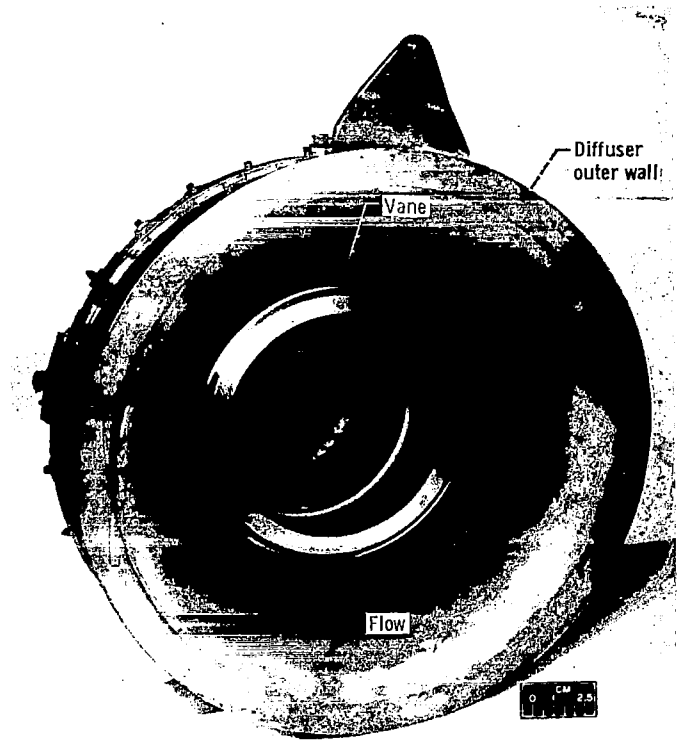

(a) Stator assembly and diffuser outer wall.

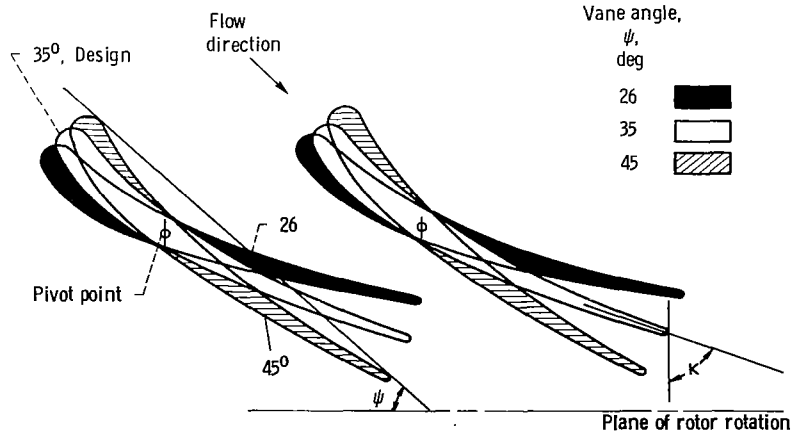

(b) Stator-vane setting angles.

Figure 2. - Stator characteristics.

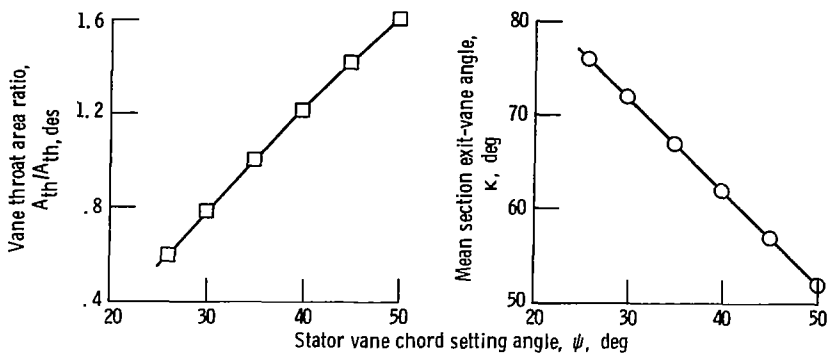

(c) Vane throat area.

(d) Mean-section exit vane angle.

Figure 2. - Concluded.

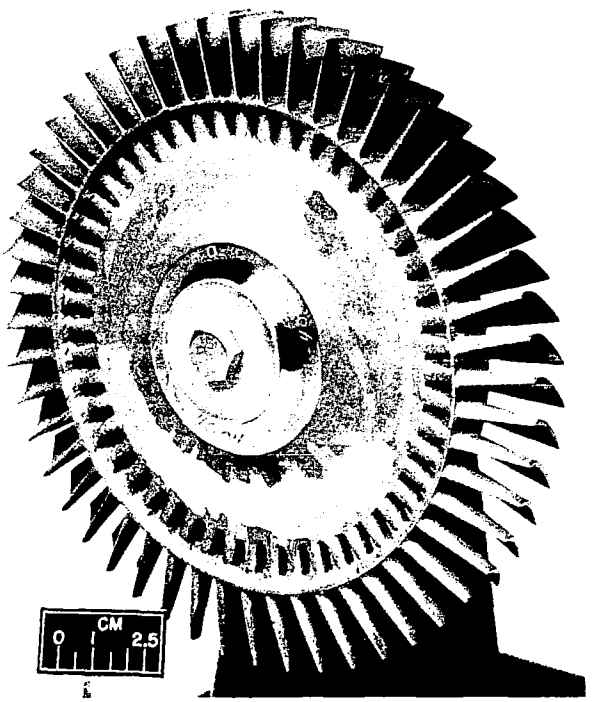

Figure 3. - Turbine rotor.

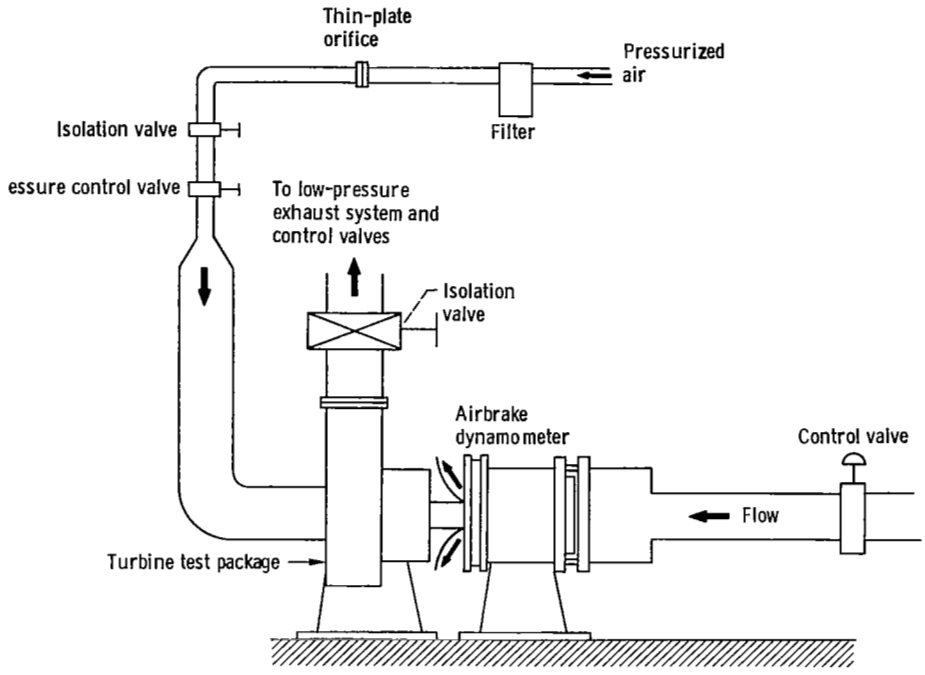

(a) Arrangement of piping and test equipment.

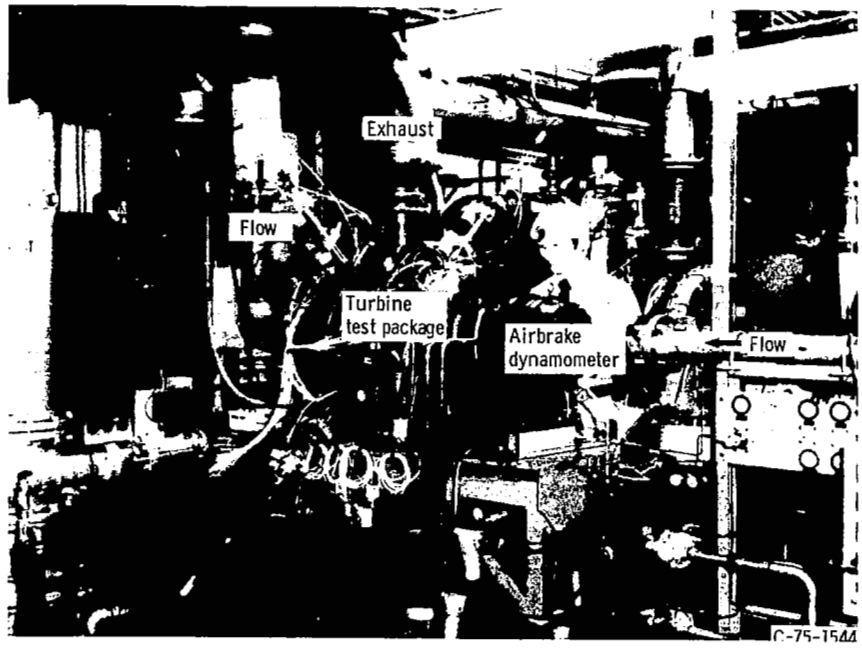

(b) Turbine test apparatus.

Figure 4. - Experimental equipment.

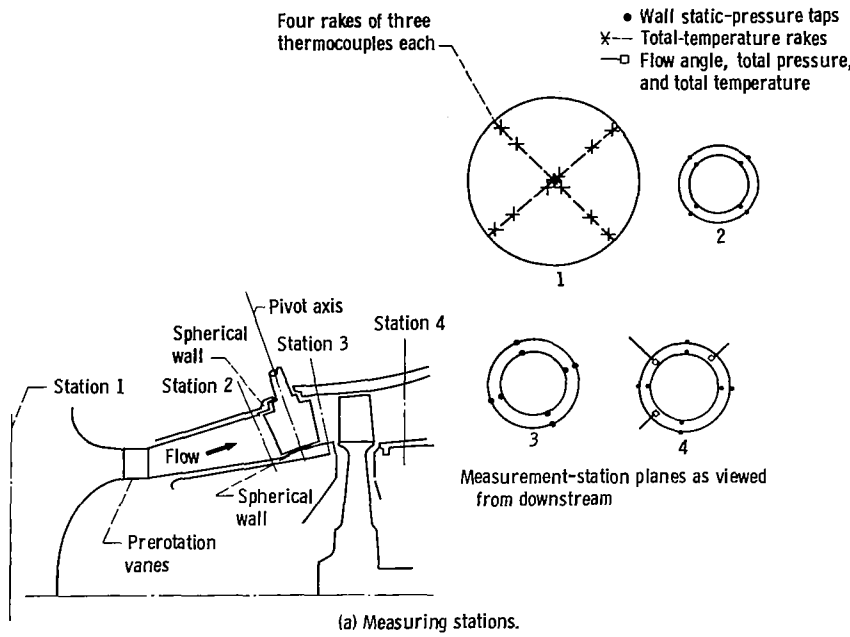

(a) Measuring stations.

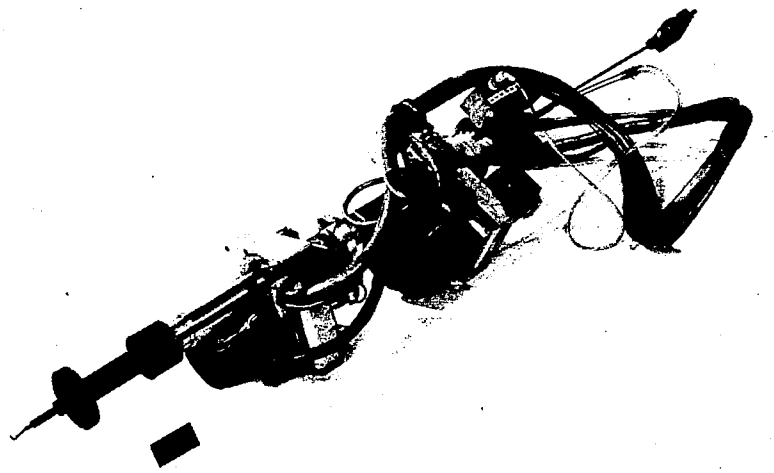

C-76-243

(b) Actuator, balance capsule, and probe assembly.

C-76-246

(c) Total pressure, total temperature, flow angle probe.

Figure 5. - Instrumentation.

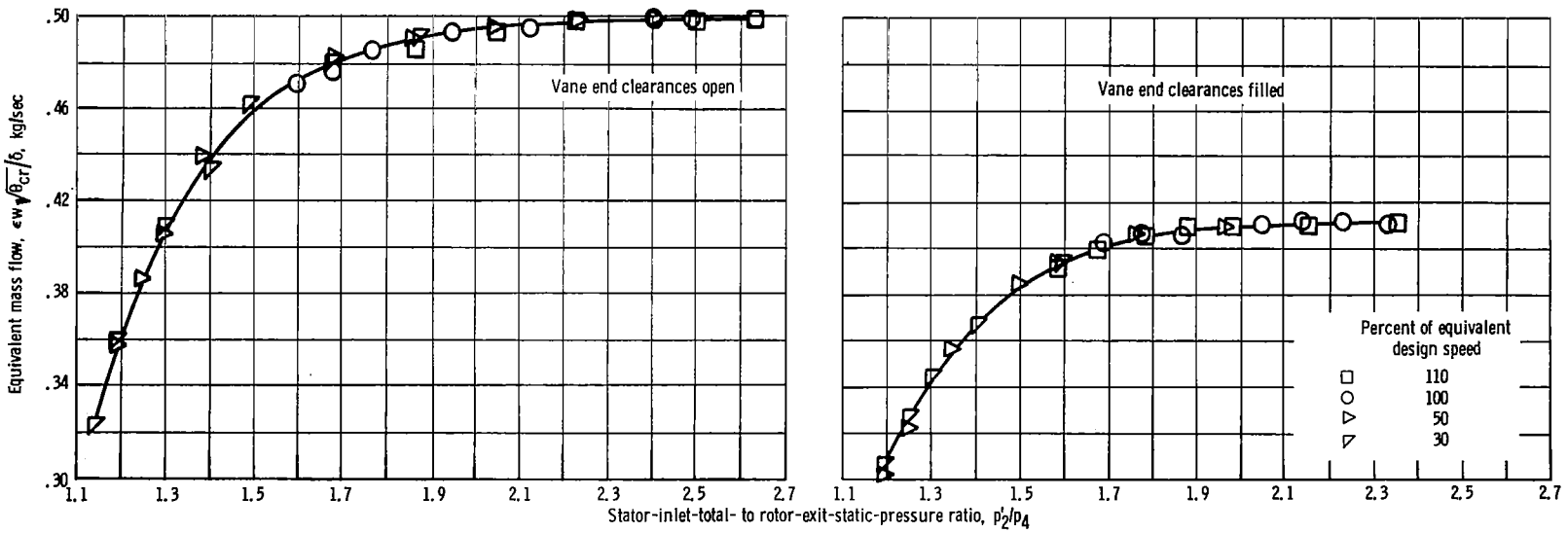

(a) Vane angle, ψ, 26^0.

Figure 6. - Variation of mass flow over range of rotative speeds and pressure ratios. (Data for open end clearances from ref. 3.)

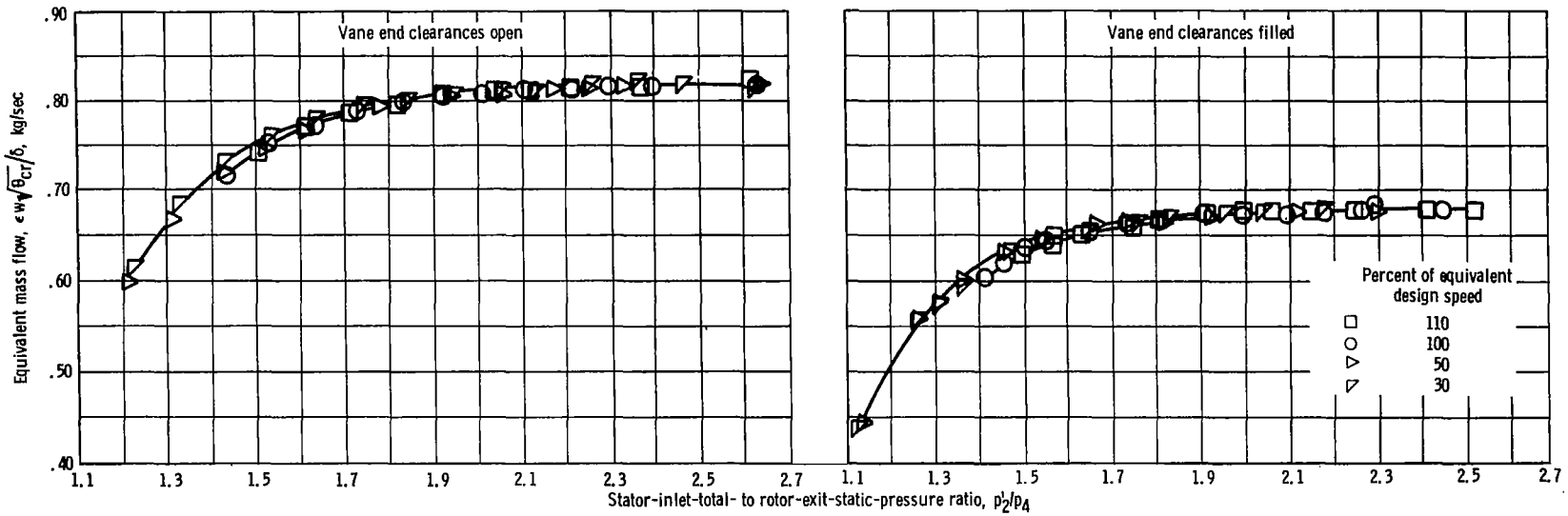

(b) Vane angle, ψ, 30°.

Figure 6. - Continued.

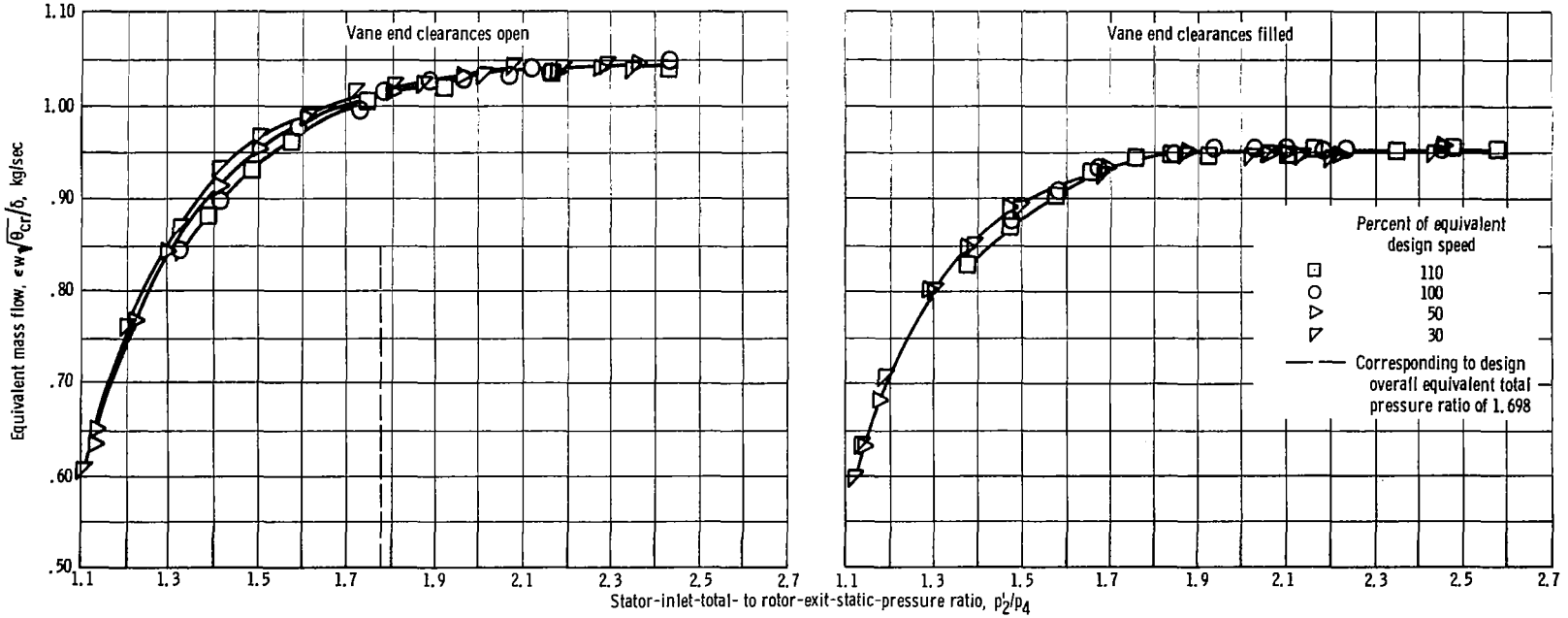

(c) Vane angle, ψ, 35°.

Figure 6. - Continued.

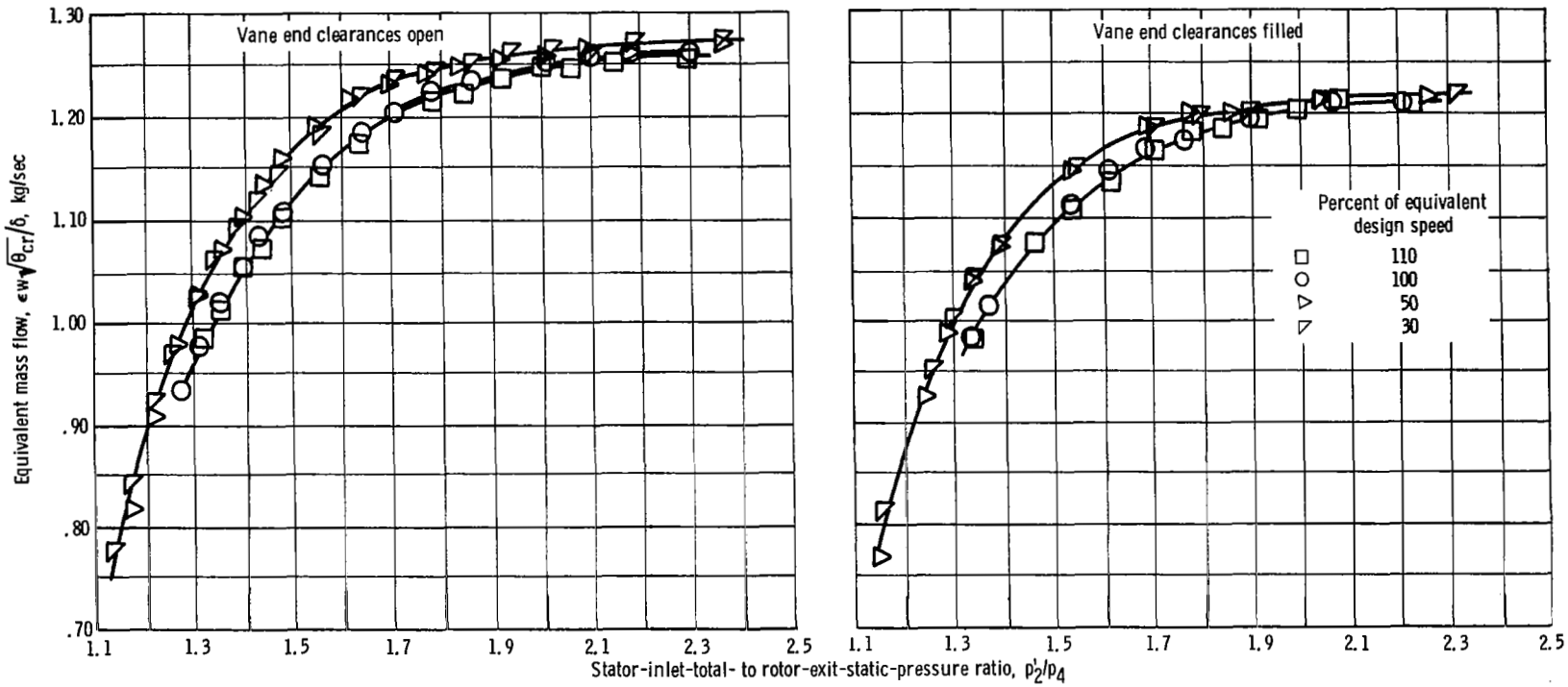

(d) Vane angle, ψ, 40°.

Figure 6. - Continued.

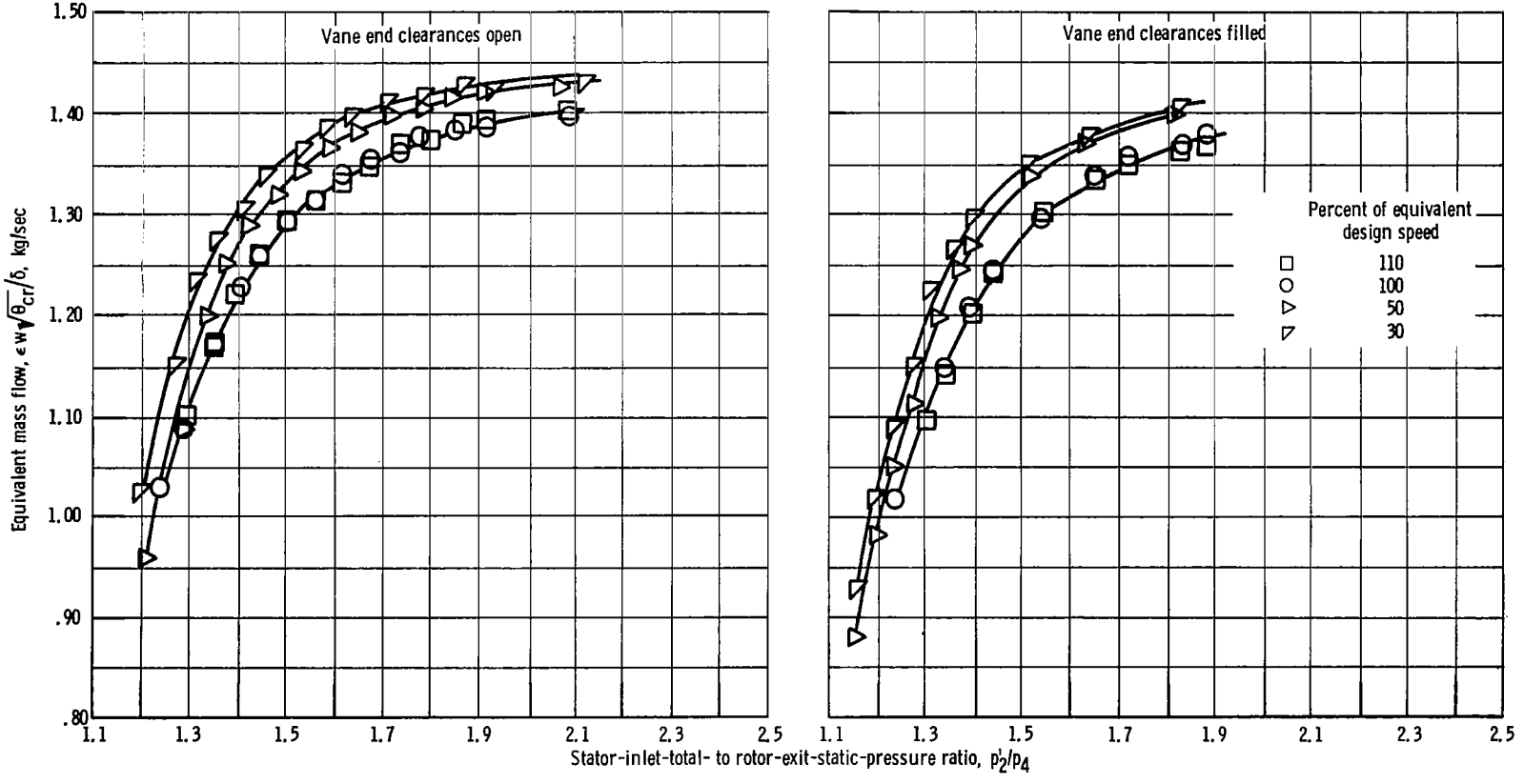

(e) Vane angle, ψ, 45^0.

Figure 6. - Continued.

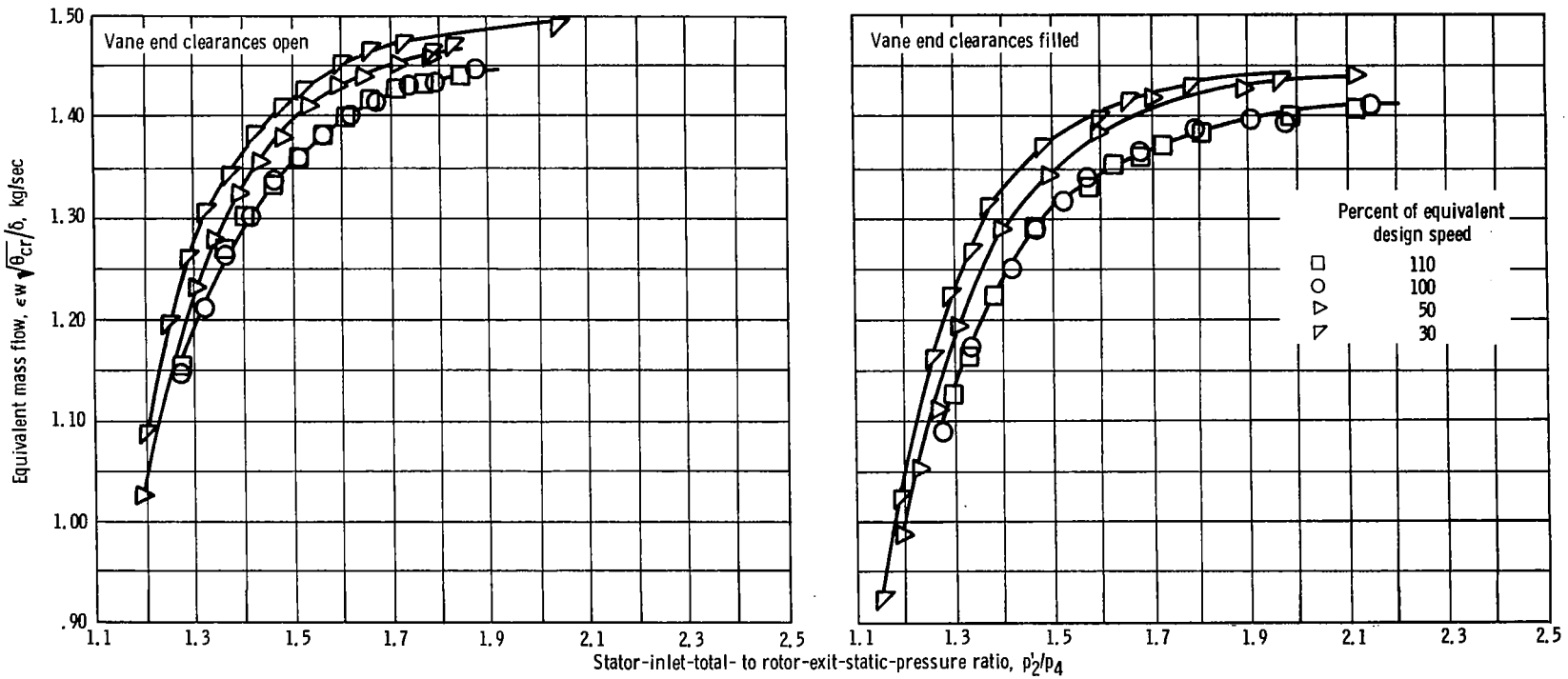

(f) Vane angle, ψ, 50^0.

Figure 6. - Concluded.

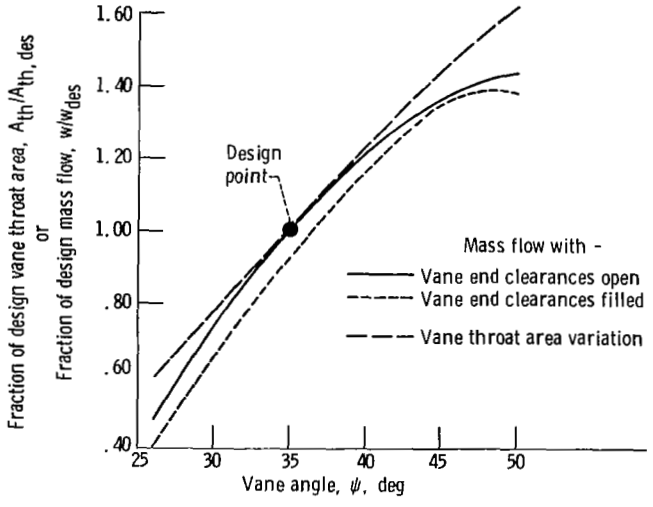

Figure 7. - Effect of vane angle and vane end clearances on mass flow. Design equivalent speed; pressure ratio (p_2'/p_4'), 1.680. (Data for open end clearances from ref. 3.)

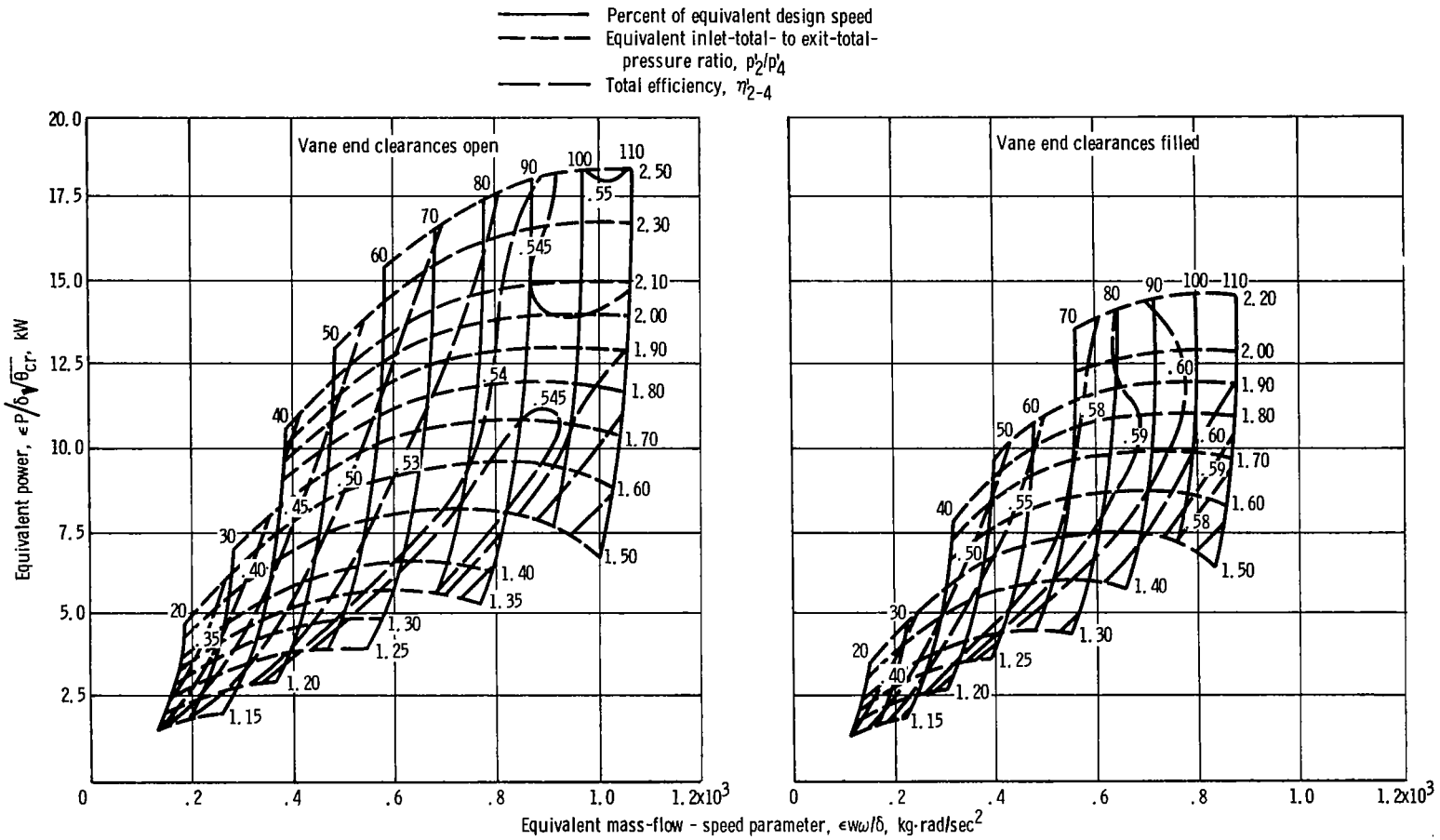

(a) Vane angle, ψ, 26°.

Figure 8. - Turbine performance map based on total conditions. (Data for open end clearance from ref. 3.)

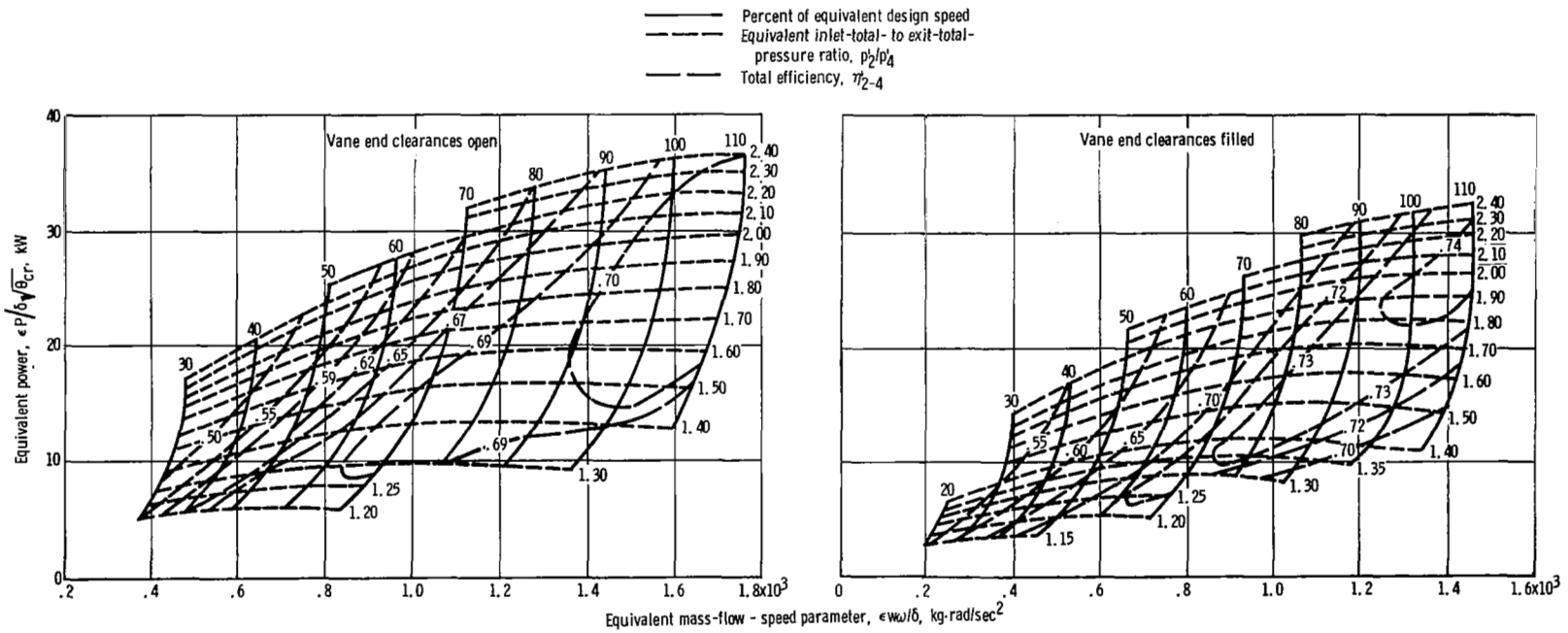

(b) Vane angle, ψ, 30°.

Figure 8. - Continued.

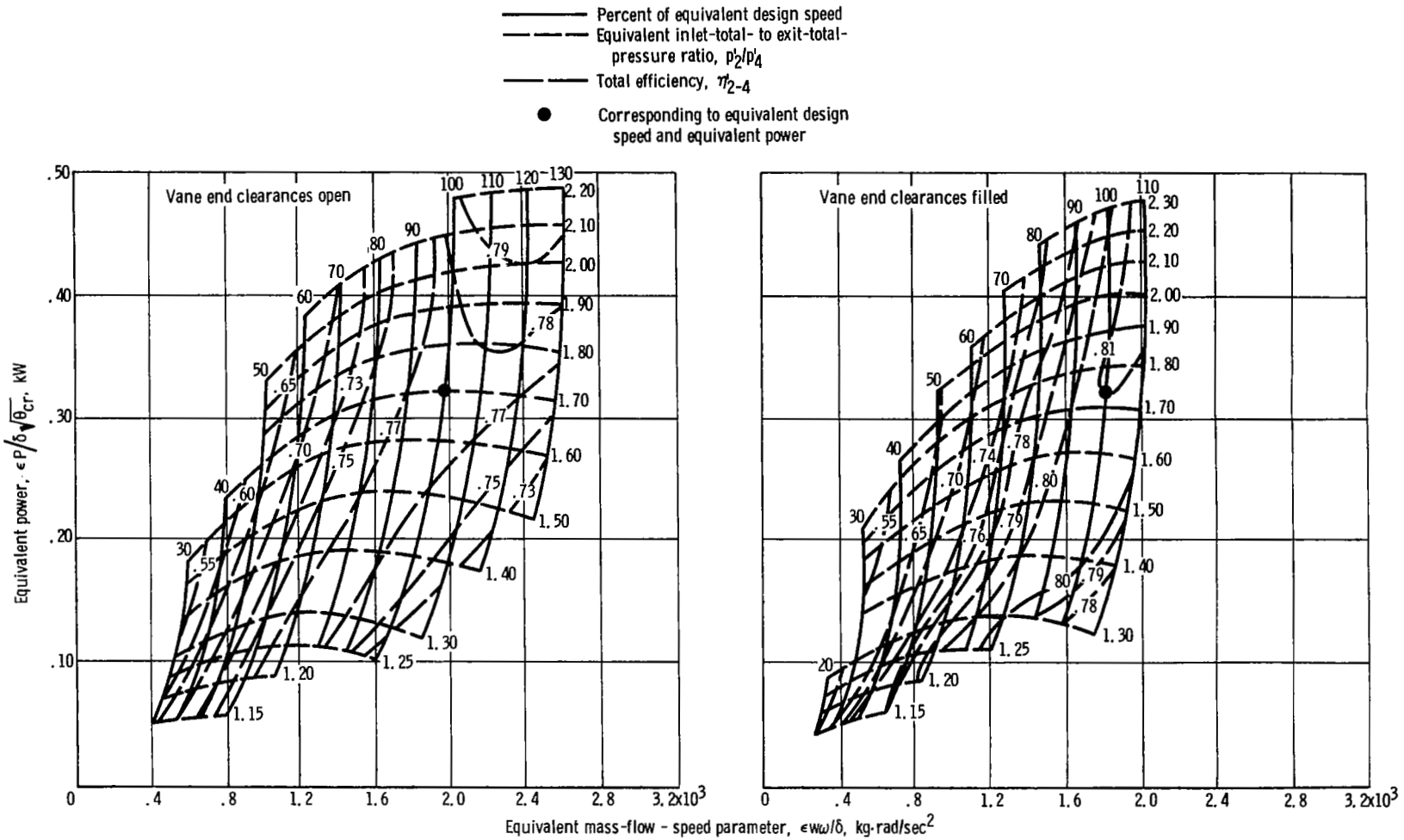

(c) Vane angle, ψ, 35°.

Figure 8. - Continued.

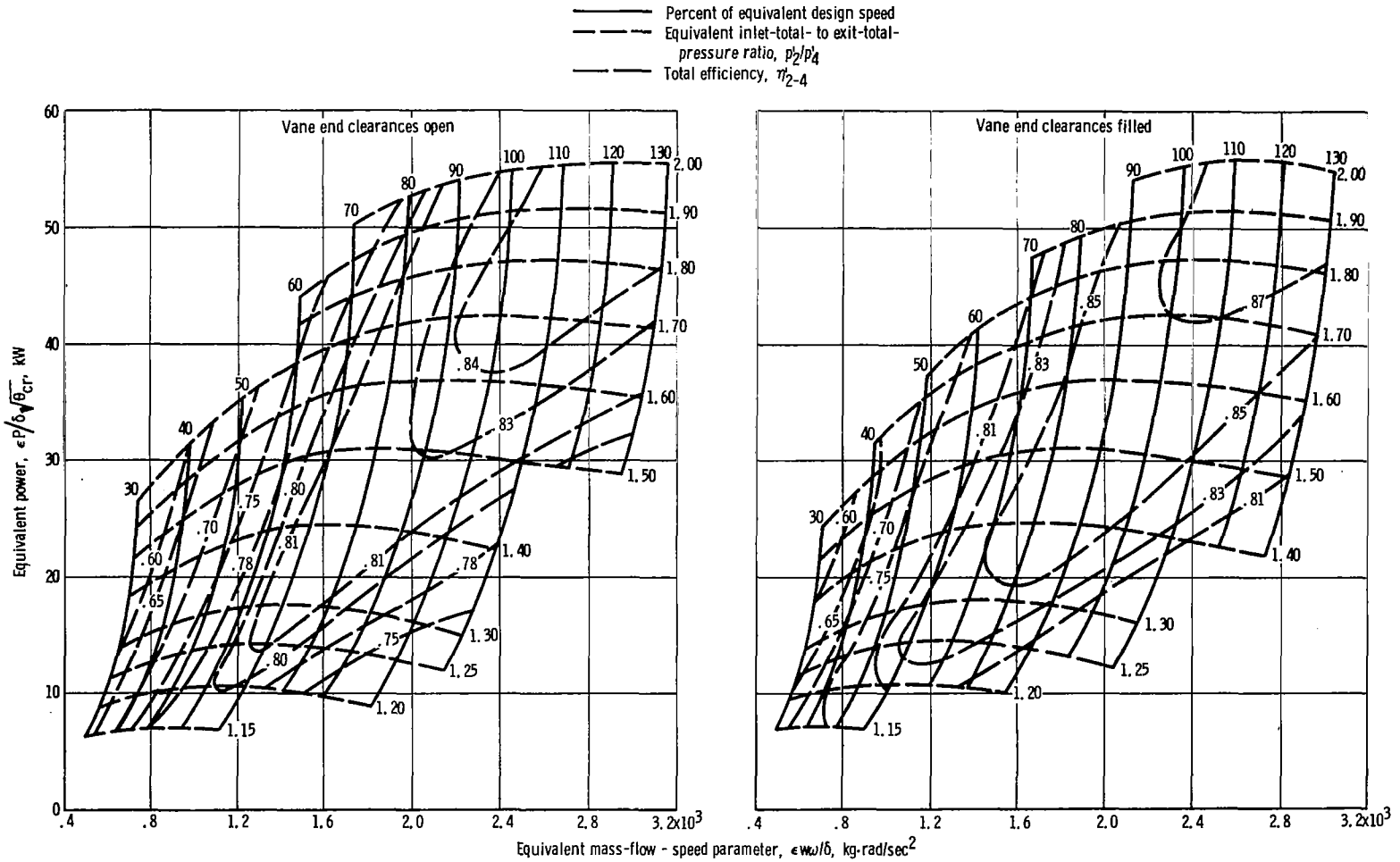

(d) Vane angle, ψ, 40^0

Figure 8. - Continued.

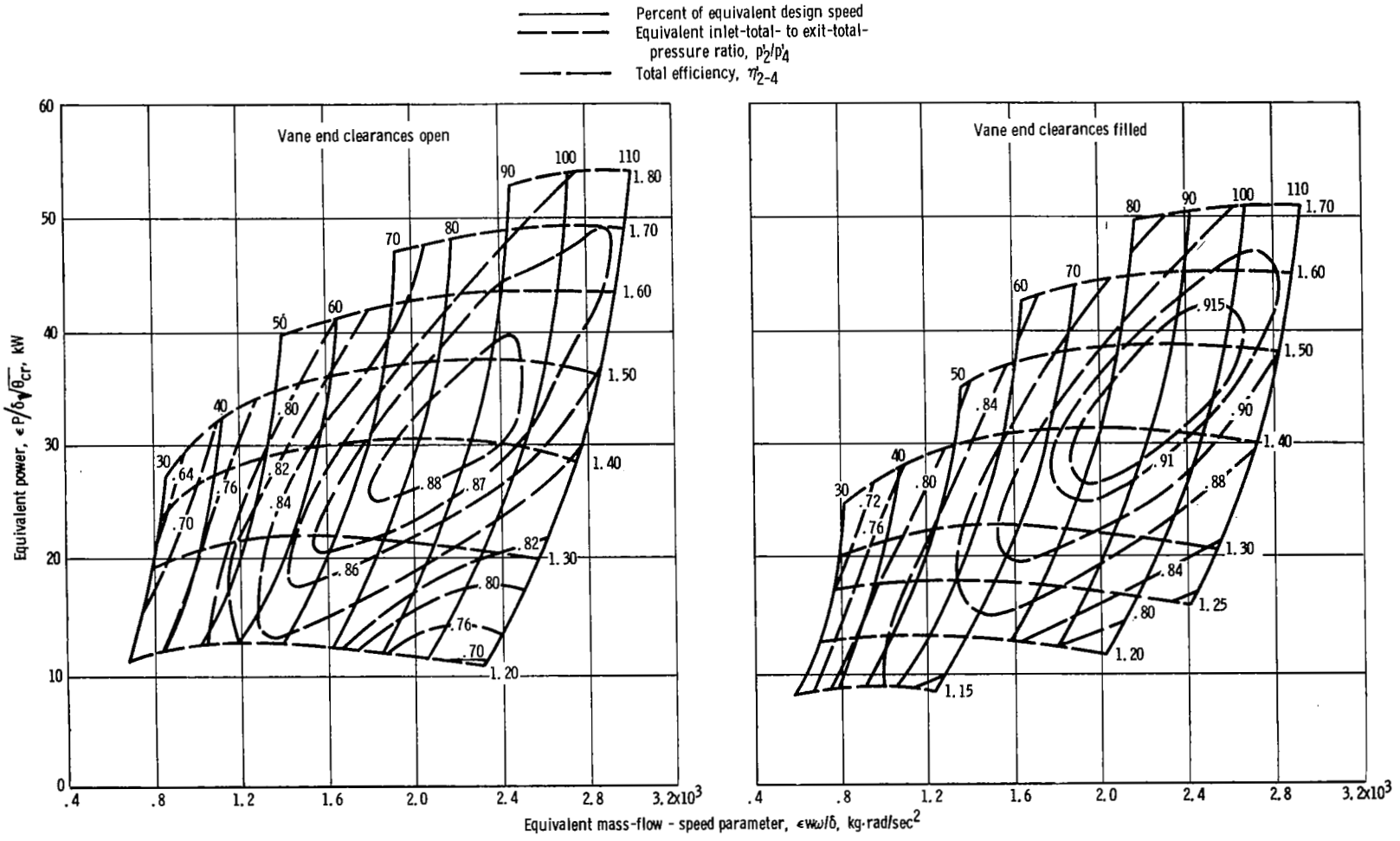

(e) Vane angle, ψ, 45°.

Figure 8. - Continued.

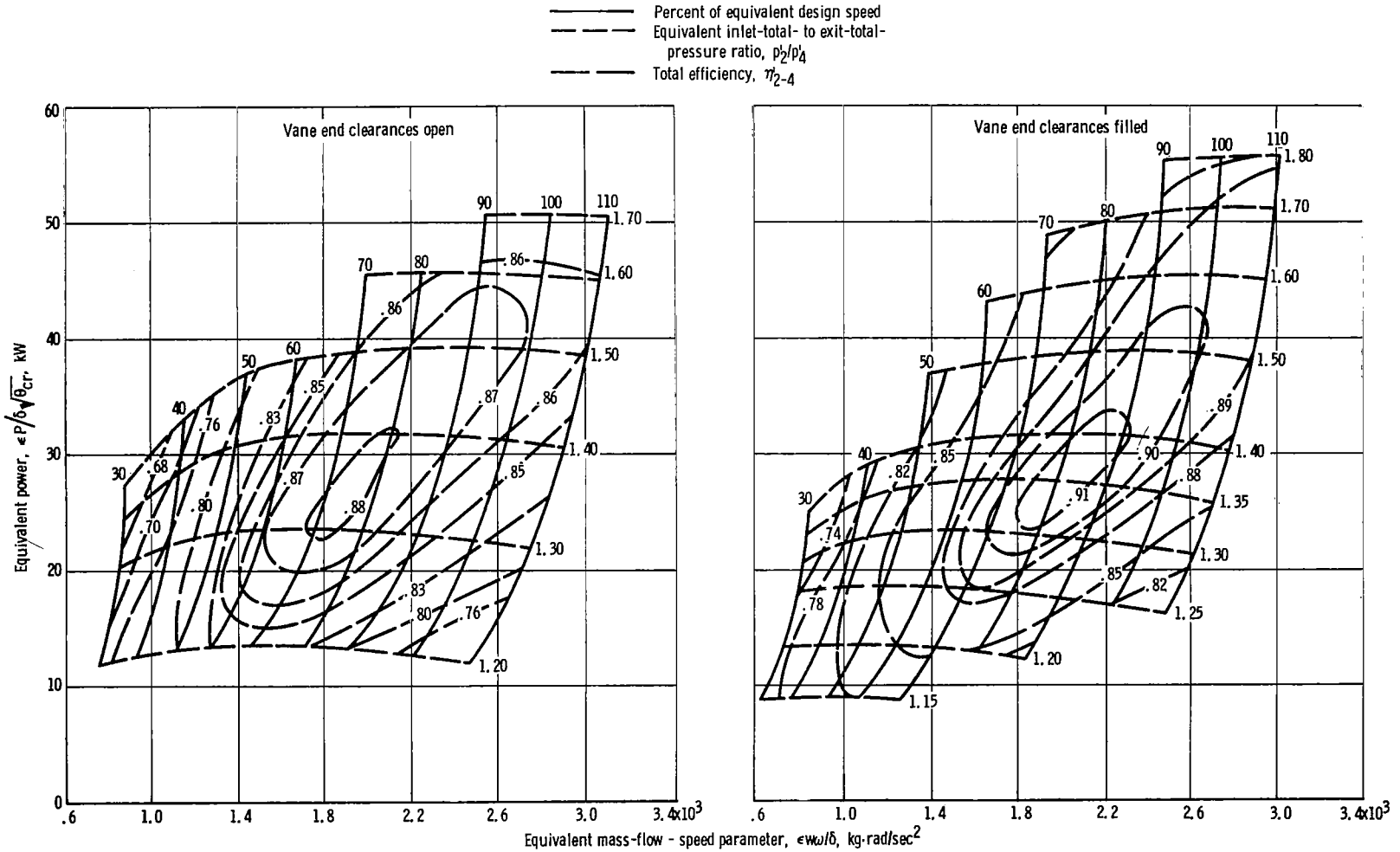

(f) Vane angle, ψ, 50°.

Figure 8. - Concluded.

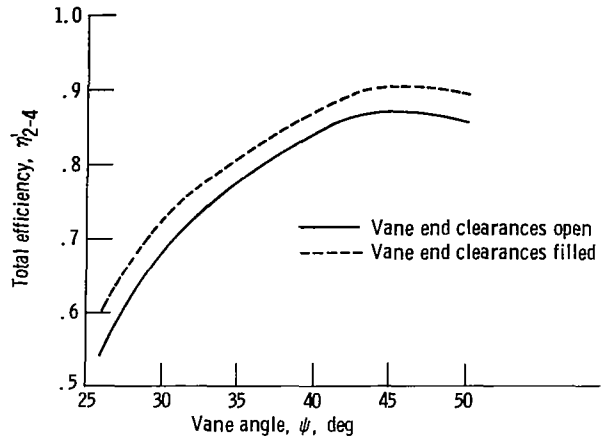

Figure 9. - Variation of turbine total efficiency as function of vane angle. Design equivalent speed and pressure ratio. (Data for open end clearance from ref. 3.)

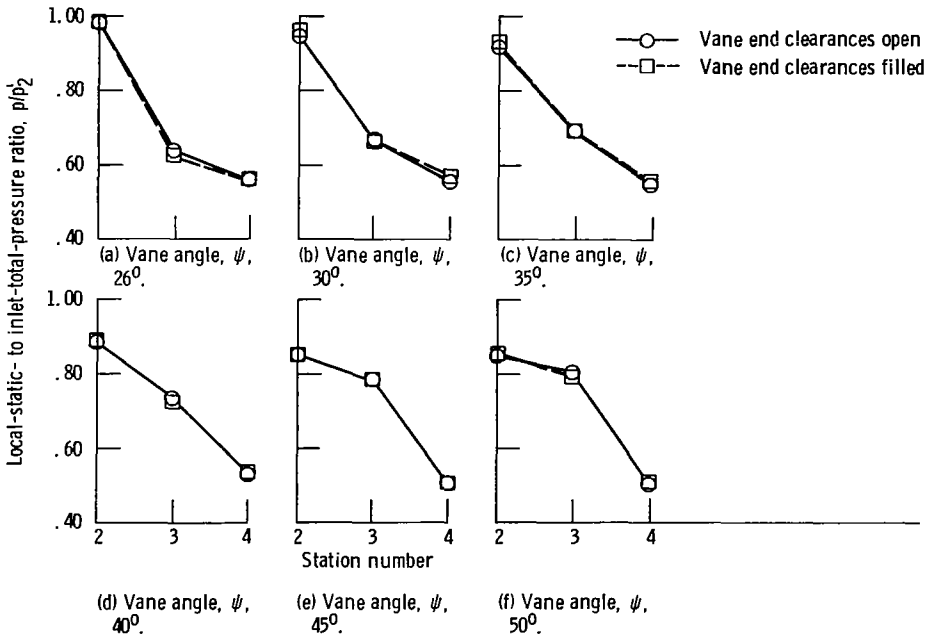

Figure 10. - Comparison of outer wall static-pressure variation through turbine. Design equivalent speed; total pressure ratio, 1.680. (Data for open end clearance from ref. 3.)

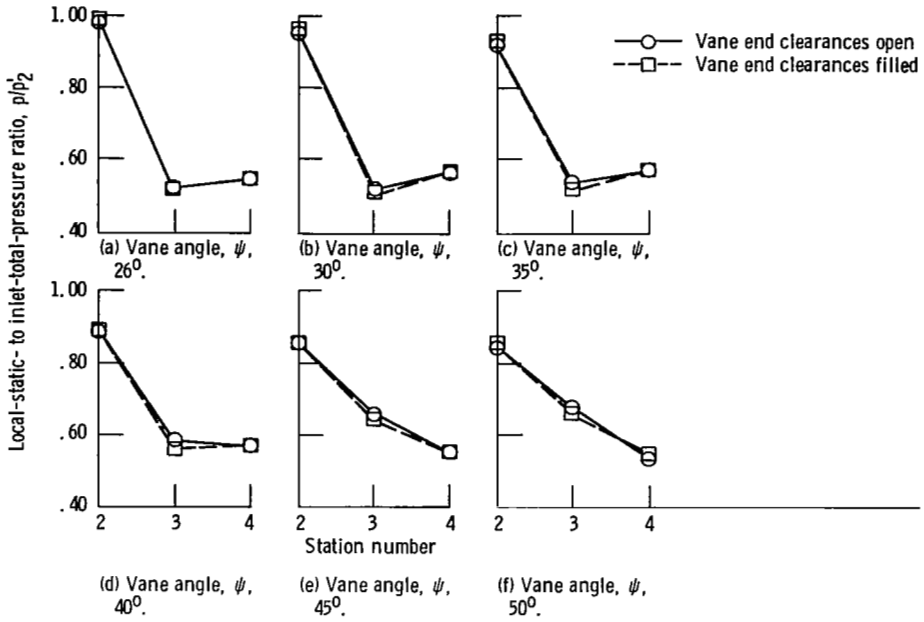

Figure 11. - Comparison of inner wall static-pressure variation through turbine. Design equivalent speed; total pressure ratio, 1.680. (Data for open end clearance from ref. 3.)

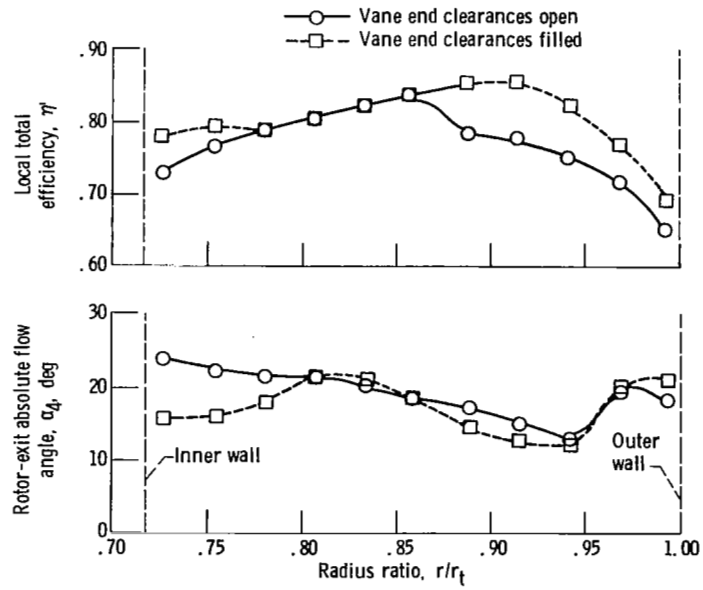

Figure 12. - Radial variations of local total efficiency and rotor-exit absolute flow angle for two end clearance conditions. Design equivalent values of speed and pressure ratio; design vane angle of 35°. (Data for open end clearance from ref. 3.)

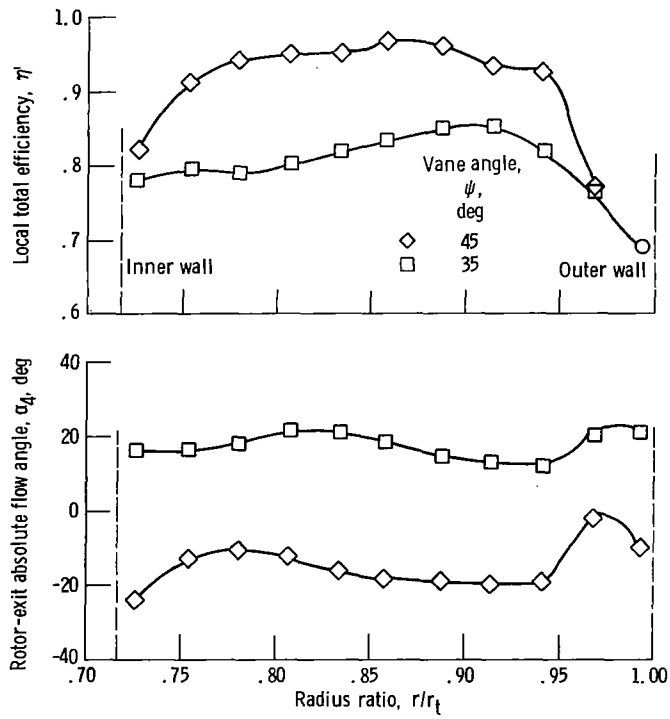

Figure 13. - Radial variations of local total efficiency and rotor-exit absolute flow angle for two vane angles. Design equivalent values of speed and pressure ratio; vane end clearances filled.

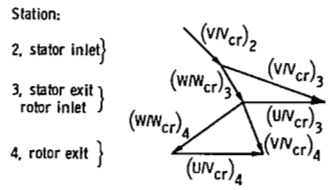

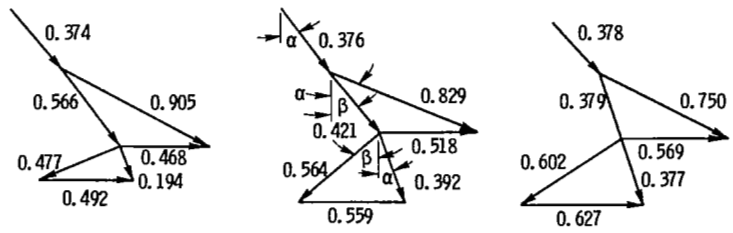

	Radius, cm		
Station 2	6.160	7.237	8.313
Station 3	7.483	8.288	9.093
Station 4	7.419	8.445	9.527
	Angle, deg		
α_2	39.5	43.5	40.2
α_3	61.7	67.5	61.8
β_3	37.5	38.0	14.6
α_4	22.6	18.5	19.5
β_4	66.8	49.5	54.7

(a) Vane end clearances open (from ref. 3).

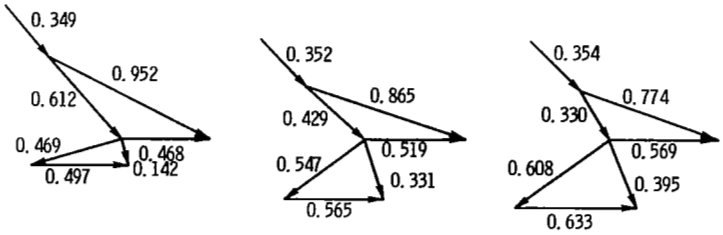

	Radius, cm		
Station 2	6.160	7.237	8.313
Station 3	7.483	8.288	9.093
Station 4	7.419	8.445	9.527
	Angle, deg		
α_2	40.9	43.0	43.8
α_3	61.9	71.4	69.1
β_3	39.6	47.5	29.3
α_4	16.2	18.7	20.2
β_4	73.4	55.7	53.3

(b) Vane end clearances filled.

Figure 14. - Velocity diagrams calculated from experimental results. Design equivalent values of speed and pressure ratio; design vane angle, ψ, 35^0.

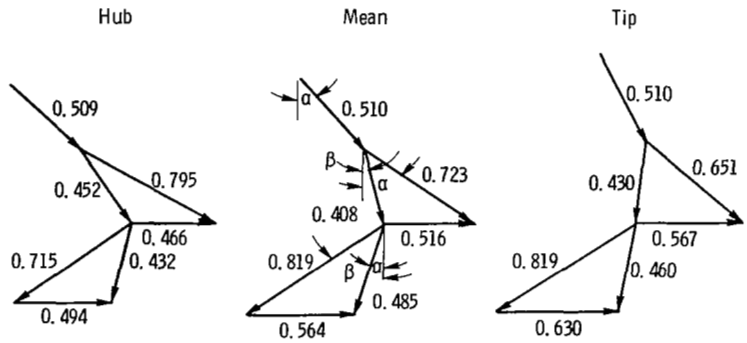

	Radius, cm		
Station 2	6.160	7.237	8.313
Station 3	7.483	8.288	9.093
Station 4	7.419	8.445	9.527
	Angle, deg		
α_2	47.1	42.1	26.1
α_3	62.8	58.0	50.3
β_3	33.5	15.4	9.0
α_4	13.1	18.3	12.0
β_4	54.6	57.3	58.2

Figure 15. - Velocity diagrams calculated from experimental results. Design equivalent speed and pressure ratio; vane angle, ψ, 45^{0}; vane end clearances filled.

1. Report No.	2. Government Accession No.	3. Recipient's Catalog No.
NASA TM-78956		

4. Title and Subtitle	5. Report Date
COLD-AIR PERFORMANCE OF FREE POWER TURBINE DESIGNED FOR 112-KILOWATT AUTOMOTIVE GAS-TURBINE ENGINE III - EFFECT OF STATOR VANE END CLEARANCES ON PERFORMANCE	December 1978
	6. Performing Organization Code
7. Author(s)	8. Performing Organization Report No.
Milton G. Kofskey and Kerry L. McLallin	E-9707
	10. Work Unit No. 778-32
9. Performing Organization Name and Address	11. Contract or Grant No.
National Aeronautics and Space Administration Lewis Research Center Cleveland, Ohio 44135	
	13. Type of Report and Period Covered
12. Sponsoring Agency Name and Address	Technical Memorandum
U.S. Department of Energy Division of Transportation Energy Conservation Washington, D.C. 20545	14. Sponsoring Agency Code Rept. No. DOE/NASA/1011-78/29

15. Supplementary Notes

Final report. Prepared under Interagency Agreement No. EC-77-A-31-1011.

16. Abstract

An experimental cold-air investigation of a turbine with a variable stator, designed for a 112-kW, automotive, gas-turbine engine was made over a range of stator-vane angles to determine the penalty in performance due to the vane end clearances. Results are presented in terms of total efficiency and mass flow for the range of vane angles from 26^{o} to 50^{o}.

17. Key Words (Suggested by Author(s))	18. Distribution Statement
Turbine engines; Automotive engines; Axial flow turbines; Single stage turbines; Gas turbines; Variable stator	Unclassified - unlimited STAR Category 07 DOE Category UC-96

19. Security Classif. (of this report)	20. Security Classif. (of this page)	21. No. of Pages	22. Price*
Unclassified	Unclassified	39	A03

* For sale by the National Technical Information Service, Springfield, Virginia 22161

NASA-Langley, 1978

National Aeronautics and Space Administration

Washington, D.C.
20546

Official Business
Penalty for Private Use, $300

THIRD-CLASS BULK RATE

Postage and Fees Paid
National Aeronautics and Space Administration
NASA-451

U.S.MAIL

22 1 1U,A, 121278 S00903DS
DEPT OF THE AIR FORCE
AF WEAPONS LABORATORY
ATTN: TECHNICAL LIBRARY (SUL)
KIRTLAND AFB NM 87117

NASA

POSTMASTER: If Undeliverable (Section 158 Postal Manual) Do Not Return